Molecular Pharmacology Fast Forward. Published on February 10, 2014 as doi:10.1124/mol.113.091249
This article has not been copyedited and formatted. The final version may differ from this version.

Molecular basis for selective serotonin re-uptake inhibition by the antidepressant agent fluoxetine (Prozac)

Jacob Andersen, Nicolai Stuhr-Hansen, Linda Grønborg Zachariassen, Heidi Koldsø, Birgit Schiøtt, Kristian Strømgaard and Anders S. Kristensen

Department of Drug Design and Pharmacology, University of Copenhagen, Universitetsparken 2, DK-2100 Copenhagen, Denmark (JA, NSH, LGZ, KS, ASK); and Center for Insoluble Structures (*in*SPIN) and Interdisciplinary Nanoscience Center (*i*NANO), Department of Chemistry, Aarhus University, Langelandsgade 140, DK-8000 Aarhus C, Denmark (HK, BS).

Molecular Pharmacology Fast Forward. Published on February 10, 2014 as DOI: 10.1124/mol.113.091249
This article has not been copyedited and formatted. The final version may differ from this version.

Running title:

The fluoxetine binding site in human SERT

Corresponding author information:

Jacob Andersen

Department of Drug Design and Pharmacology, University of Copenhagen, Universitetsparken 2, DK-2100 Copenhagen, Denmark.

E-mail: jaa@sund.ku.dk. Tel.: +45 3533 6388. Fax: +45 3533 6040.

Text pages: 15

Tables: 2

Figures: 6

References: 50

Abstract: 224 words

Introduction: 747 words

Discussion: 1489 words

Abbreviations used:

5-HT: 5-hydroxytryptamine, serotonin; β-CIT: (-)-2β-carbomethoxy-3β-(4-iodophenyl)tropane; DAT: dopamine transporter; IFD: induced-fit docking; NET: norepinephrine transporter; RMSD: root-mean-square deviation; SERT: serotonin transporter; SSRI: selective serotonin reuptake inhibitor; TCA: tricyclic antidepressant.

Molecular Pharmacology Fast Forward. Published on February 10, 2014 as DOI: 10.1124/mol.113.091249
This article has not been copyedited and formatted. The final version may differ from this version.

ABSTRACT

Inhibitors of the serotonin transporter (SERT) are widely used antidepressant agents, but the structural mechanism for inhibitory activity and selectivity over the closely related norepinephrine transporter (NET) is not well understood. Here we use a combination of chemical, biological and computational methods to decipher the molecular basis for high-affinity recognition in SERT and selectivity over NET for the prototypical antidepressant drug fluoxetine (Prozac). We show that fluoxetine binds within the central substrate site of human SERT, in agreement with recent X-ray crystal structures of LeuBAT, an engineered monoamine-like version of the bacterial amino acid transporter LeuT. However, the binding orientation of fluoxetine is reversed in our experimentally supported model compared to the LeuBAT structures, emphasizing that need for careful experimental verification when extrapolating findings from crystal structures of bacterial transporters to human relatives. We find that the selectivity of fluoxetine and nisoxetine, a NET selective structural congener of fluoxetine, is controlled by residues in different regions of the transporters, indicating a complex mechanism for selective recognition of structurally similar compounds in SERT and NET. Our findings add important new information on the molecular basis for SERT/NET selectivity of antidepressants, and provide the first assessment of the potential of LeuBAT as a model system for antidepressant binding in human transporters which is essential for future structure-based drug development of antidepressant drugs with fine-tuned transporter selectivity.

Molecular Pharmacology Fast Forward. Published on February 10, 2014 as DOI: 10.1124/mol.113.091249
This article has not been copyedited and formatted. The final version may differ from this version.

INTRODUCTION

The early recognition of the serotonin (5-hydroxytryptamine; 5-HT) transporter (SERT) and the norepinephrine transporter (NET) as important targets for antidepressant drugs, fostered extensive drug discovery efforts dedicated to the design and synthesis of compounds selectively targeting SERT and/or NET (Kristensen et al., 2011). In 1986, fluoxetine (Prozac) was approved as one of the first selective serotonin re-uptake inhibitors (SSRIs) for the treatment of depression, and has since then become widely acknowledged as a breakthrough drug for depression (Wong et al., 1995; Wong et al., 2005). Unlike the tricyclic antidepressants (TCAs), fluoxetine and other SSRI drugs are highly selective for SERT and today the SSRIs remain among the most widely prescribed antidepressant drugs (Bauer et al., 2008; Waitekus and Kirkpatrick, 2004).

Although compounds targeting SERT and NET have had important clinical significance for several decades, the molecular details underlying binding of antidepressants to these transporters are not clearly understood. Structural information of SERT and NET is still lacking, but X-ray crystal structures of the bacterial homolog LeuT (Krishnamurthy and Gouaux, 2012; Yamashita et al., 2005) have proved to be excellent structural templates for its mammalian counterparts and facilitated identification of the location and structure of ligand binding sites in human transporters (Andersen et al., 2010; Andersen et al., 2009; Beuming et al., 2008; Celik et al., 2008; Kaufmann et al., 2009; Koldsø et al., 2013a; Koldsø et al., 2010; Plenge et al., 2012; Severinsen et al., 2013; Severinsen et al., 2012; Sinning et al., 2010). Structures of LeuT have also provided direct insight into the binding mechanism of antidepressants. SSRIs and TCAs bind LeuT with low affinity to a site (denoted S2) located in an extracellular facing vestibule (Fig. 1) (Singh et al., 2007; Zhou et al., 2007; Zhou et al., 2009), leading to the proposal that antidepressant drugs also bind to the S2 site in human transporters (Zhou et al., 2007; Zhou et al., 2009). In contrast, recent structures of LeuBAT, an engineered version of LeuT with residues from SERT inserted into the central substrate site (denoted S1), and the dopamine transporter (DAT) from *Drosophila melanogaster*, displayed high-affinity binding of antidepressants within the central S1 site (Fig. 1) (Penmatsa et al., 2013; Wang et al., 2013). Combined with biochemical studies showing that most SSRIs inhibit SERT in a competitive manner (Apparsundaram et al.,

Molecular Pharmacology Fast Forward. Published on February 10, 2014 as DOI: 10.1124/mol.113.091249
This article has not been copyedited and formatted. The final version may differ from this version.

2008; Graham et al., 1989; Koe et al., 1990), and several residues located within the S1 site of SERT and NET have been shown to be important for binding of SSRIs (Andersen et al., 2010; Andersen et al., 2009; Barker et al., 1999; Henry et al., 2006; Koldsø et al., 2010; Mason et al., 2007; Sørensen et al., 2012; Walline et al., 2008), LeuBAT and *Drosophila* DAT seem to represent improved structural frameworks for studying the molecular pharmacology of human transporters compared to LeuT.

Fluoxetine has been co-crystallized together with both LeuT and LeuBAT, and these studies have provided ambiguous insight into the binding mechanism of this important SSRI drug. Whereas fluoxetine binds to the S2 site in LeuT it binds to the S1 site in LeuBAT (Fig. 1) (Wang et al., 2013; Zhou et al., 2009). Surprisingly few biochemical studies have addressed the location of the fluoxetine binding site in human SERT, but is has been found that binding of fluoxetine is chloride-dependent and highly sensitive towards mutation of Ile172 to Met (Henry et al., 2006; Sørensen et al., 2012; Tavoulari et al., 2009; Walline et al., 2008). As Ile172 and the chloride binding site are both located within the central part of SERT, these observations are consistent with the S1 binding mode found in LeuBAT. However, both effects have been proposed to be allosterically induced (Tavoulari et al., 2009; Walline et al., 2008), and do thus not unequivocally pinpoint the location of the fluoxetine binding site. In contrast, nisoxetine, a structural congener of fluoxetine with selectivity for NET, was recently proposed to bind in the S2 site of NET (Wang et al., 2012). Given the structural similarity between nisoxetine and fluoxetine (Fig. 1) it is tempting to believe that they share the same binding site in SERT and NET, respectively. Here we have used a combination of chemical, biological and computational approaches to decipher the molecular basis for binding of fluoxetine in SERT and selectivity over NET. Our study finds that fluoxetine bind within the S1 site of SERT and allow for the first assessment of LeuBAT as a model system for directly revealing the binding mode of antidepressants in human transporters.

MATERIALS AND METHODS

Synthesis. A complete description of the synthesis and full characterization of fluoxetine, nisoxetine and analogs **7**-**11** are found in *Supplementary Methods.*

Molecular Pharmacology Fast Forward. Published on February 10, 2014 as DOI: 10.1124/mol.113.091249
This article has not been copyedited and formatted. The final version may differ from this version.

Molecular biology. As expression vectors, pcDNA3.1 and pCI-IRES-neo containing human SERT and NET, respectively, were used (Andersen et al., 2011; Kristensen et al., 2004). Generations of point-mutants in SERT and NET was performed by site-directed mutagenesis using the QuickChange mutagenesis kit (Stratagene). Multiple mutants were generated by introducing one or more mutations into existing mutants using site-directed mutagenesis. The mutations were verified by DNA sequencing of the entire gene (GATC Biotech). Synthetic cDNA encoding the two 15-fold mutants SERT-(NET S1) and NET-(SERT S1) were purchased from GeneArt, and subcloned into the pCI-IRES-neo expression vector as detailed previously (Andersen et al., 2011).

Transport assays and radioligand binding experiments. [^{3}H]5-HT and [^{3}H]dopamine uptake measurements in COS7 cells expressing wild-type (WT) and mutant forms of SERT and NET and binding of [^{125}I]-labeled (-)-2β-carbomethoxy-3β-(4-iodophenyl)tropane (β-CIT) to membranes of COS7 cells expressing WT and mutant forms of SERT and NET was performed essentially as described (Andersen et al., 2011; Sørensen et al., 2012). A detailed description of the functional uptake assay and radioligand binding assay are provided in Supplemental Methods.

Computational methods. The *R*- and *S*-enantiomers of fluoxetine were docked into homology models of human SERT and NET, which was generated and validated as described previously (Koldsø et al., 2013b). To allow for protein flexibility during docking calculations, the induced-fit docking (IFD) workflow within the Schrödinger software suite (Schrödinger Suite 2011 Induced Fit Docking protocol; Sherman et al., 2006) was utilized. To address the binding of fluoxetine both in the central S1 site and the S2 site in the extracellular facing vestibule, two different types of IFD calculations were set up for each transporter. *R*- and *S*-fluoxetine were docked into the transporters utilizing the endogenous substrate bound to the S1 site as the binding site definition with the default settings for the size of the binding site (an 26×26×26 Å^3 box as outer boundary for ligand and an inner box of 10×10×10 Å^3 which should include the center of the ligand). These IFDs are termed small. In separate calculations, IFDs were performed where the binding site was defined from residues within the S1 site (SERT: Asp98 and Ile172. NET: Asp75 and Val148) in addition to S2 site residues (SERT: Arg104 and Glu493. NET: Arg81 and Asp473). In these IFDs, which are termed large, the inner box dimensions were increased to 20×20×20 Å^3. Additionally Trp80 of NET was mutated to Ala

Molecular Pharmacology Fast Forward. Published on February 10, 2014 as DOI: 10.1124/mol.113.091249
This article has not been copyedited and formatted. The final version may differ from this version.

during the initial docking stage since this residue was blocking the S2 site. The aligning residue in SERT (Trp103) is pointing away from the S2 site in the homology model and accordingly there was no need for mutation of this residue during initial docking. The maximum number of output structures was set to 20, and the recovered binding poses were ranked according to their GScore and Emodel score. The GScore is an empirical scoring function that accounts for the interaction energy between the ligand and the protein and approximates the ligand binding free energy while the Emodel score is a combination of the GScore, the nonbonded interactions, and the internal strain of the ligand (Friesner et al., 2004). The docking results have been divided into structural clusters based on heteroatom root-mean-square deviation (RMSD) < 2 Å in each docking. The structural clusters identified in each docking setup were further divided into global clusters. The global clusters were defined based on an RMSD < 2.3 Å between the heteroatoms of fluoxetine.

RESULTS

Structure-activity relationship study. Fluoxetine and nisoxetine share a substituted phenoxyphenylpropylamine skeleton, and are distinguished by their substitution on the phenoxy ring only. Where fluoxetine has a CF_3 group in the *para* position, nisoxetine has a methoxy group in the *ortho* position (Fig. 1). To delineate the role of these two diverging structural elements for activity at SERT and NET, we designed and prepared derivatives of fluoxetine and nisoxetine with different substituents on the phenoxy ring (Table 1) (see *Supplementary Methods*). Furthermore, the length and methyl substitution pattern of the aminoalkyl chain of SSRIs and TCAs have previously been shown to be an important determinant for activity and selectivity towards SERT and NET (Andersen et al., 2009; Owens et al., 1997). To investigate the role of the aminoethyl chain of fluoxetine for activity and selectivity towards SERT and NET, we also prepared analogs of fluoxetine with modifications around the aminoalkyl chain (Table 1) (see *Supplementary Methods*).

The binding affinities of the synthesized compounds was determined by displacing binding of the [^{125}I]-labeled cocaine analog *β*-CIT to human SERT and NET transiently expressed in membranes from COS-7 cells. As expected, fluoxetine had high affinity towards SERT and selectivity over NET (7 nM versus 887

Molecular Pharmacology Fast Forward. Published on February 10, 2014 as DOI: 10.1124/mol.113.091249
This article has not been copyedited and formatted. The final version may differ from this version.

nM), whereas nisoxetine had high affinity towards NET and selectivity over SERT (4 nM versus 167 nM) (Fig. 1 and Table 1). Hence, as recognized from early SAR studies, *ortho* substitution of the phenoxy ring appears to confer selectivity towards NET, whereas substituents in the *para* position induce selectivity towards SERT (Wong et al., 1975). However, the analog with an unsubstituted phenoxy ring (compound **8**) displayed comparable affinity towards NET as nisoxetine (4 nM versus 12 nM) whereas the analog with both *ortho* and *para* substitution (compound **9**) had similar binding affinity towards SERT as fluoxetine (7 nM versus 4 nM) (Table 1), showing that the *ortho* substituent is a minor determinant for selective binding in NET over SERT. In contrast, the CF_3 substituent is essential for high affinity binding in SERT and greatly reduces binding in NET (Table 1), thus showing that this substituent is the main determinant for the distinct selectivity profiles observed for fluoxetine and nisoxetine. In agreement with previous SAR studies of fluoxetine (Horng and Wong, 1976; Wong et al., 1975), we found that addition of an *N*-methyl group to fluoxetine (as in compound **7**) reduced affinity towards SERT (7 nM versus 37 nM) but increased the selectivity for SERT over NET (127-fold versus 286-fold). Extending the aminoalkyl chain of fluoxetine with one methylene group (as in compound **10**), had a minor effect on the affinity for SERT (7 nM versus 12 nM) but increased the selectivity over NET (127-fold versus 279-fold). The *N*,*N*-dimethyl analog of homofluoxetine (compound **11**) had low activity towards both SERT and NET. The length and substitution pattern of the aminoalkyl chain on fluoxetine is thus an important determinant for binding and SERT/NET selectivity, which has also been observed for other SSRIs and TCAs (Andersen et al., 2009; Owens et al., 1997). Fluoxetine is a racemate consisting of a 1:1 mixture of *R*- and *S*-enantiomers and, unlike other antidepressant drugs that are highly enantioselective, the two enantiomers of fluoxetine have similar binding affinities for SERT (Wong et al., 1985). We determined the binding affinities of the *R*- and *S*-enantiomers of fluoxetine at SERT and NET, and found the two enantiomers to be 389- and 108-fold selective towards SERT over NET, respectively, thereby showing that the stereochemistry of fluoxetine is an important determinant for SERT/NET selectivity (Table 1). In summary, our SAR analysis demonstrates that minor modifications of the chemical scaffold of fluoxetine can improve the affinity towards SERT and increase the selectivity over NET, whereas none of the compounds tested had greater affinity for NET or improved selectivity over SERT compared to nisoxetine.

Molecular Pharmacology Fast Forward. Published on February 10, 2014 as DOI: 10.1124/mol.113.091249
This article has not been copyedited and formatted. The final version may differ from this version.

Molecular docking. To create models of possible binding modes of fluoxetine in SERT and NET, we performed IFD calculations of *R*- and *S*-fluoxetine into homology models of human SERT and NET. The SERT and NET homology models were constructed using LeuT as template (Koldsø et al., 2013b). Previous LeuT-based models of TCA binding in human SERT (Sinning et al., 2010) have proved to be very predictive when compared with the recent structure of the eukaryotic *Drosophila* DAT in complex with the TCA nortriptyline (Penmatsa et al., 2013) (Supplemental Figure 1). Specifically, we do also observe the aromatic lid (Tyr176/Phe335) to be broken in our IFD calculations of fluoxetine in human SERT, showing that the outward-occluded LeuT structure can be used as template for human SERT and still provide an inhibitor-bound transporter model in an outward-open conformation. Furthermore, the overall structure of *Drosophila* DAT is very similar to that of LeuT, emphasizing that the LeuT-fold is conserved from prokaryotic to eukaryotic transporters, and together this substantiates the continued use of LeuT as structural template for human transporters in the study of drug binding. Initially, IFD calculations were confined to the S1 binding site of SERT and NET (denoted small IFDs). In separate runs, the entire S1/S2 region was included in the docking calculations (denoted large IFDs). The docking results have been divided into clusters based on heteroatom RMSD < 2Å, and further mapped into global clusters describing common binding modes by comparison of all clusters obtained from both small and large IFDs of both enantiomers of fluoxetine (Fig. 2 and Table 2). The global clusters were defined based on RMSD < 2.3Å between the heteroatoms of fluoxetine.

Overall, we observe three global clusters of fluoxetine binding in SERT. In the most prevalent binding mode identified in SERT-Cluster 1 (containing 89% of the poses obtained) (Table 2), fluoxetine is located almost entirely within the central S1 site except for the CF_3-substituted phenyl ring which protrudes out towards the S2 site (Fig. 2a). In agreement with the similar binding affinities of *R*- and *S*-fluoxetine for SERT (Table 1), the Gscores are also computed to be very similar for the two enantiomers. Additionally, a significant overlap between the two enantiomers in SERT-Cluster 1 is seen, where the amine of fluoxetine is anchored between Tyr95 and Asp98 on TM1, and the unsubstituted phenyl ring is located close to Ile168, Ile172 and Phe341 on TM3. Two minor global clusters of fluoxetine binding were also obtained (SERT-Cluster 2 and SERT-Cluster 3; 9% and 2%, respectively, of the poses obtained) (Table 2). In these two clusters, fluoxetine is

Molecular Pharmacology Fast Forward. Published on February 10, 2014 as DOI: 10.1124/mol.113.091249
This article has not been copyedited and formatted. The final version may differ from this version.

exclusively located in the S2 site and the amine of the ligand is located close to Glu493 from TM10 in both clusters (Fig. 2a).

From IFD calculations in NET, we also found three global clusters of fluoxetine binding. In the dominating binding mode (NET-Cluster 1; 63% of the poses obtained) (Table 2), fluoxetine is located in the S1 site below an aromatic lid (Tyr152/Phe317) (Fig. 2b). The amine of fluoxetine is coordinated by Asp75, the CF_3-substituted phenyl ring is located just above Phe72, and the unsubstituted phenyl ring is located close to Ile144, Val148 and Phe323. There is a significant overlap between the two enantiomers of fluoxetine in NET-Cluster 1, which is in agreement with the comparable binding affinities of the enantiomers towards NET (Table 1). Two minor global clusters were also obtained from IFDs in NET (NET-Cluster 2 and NET-Cluster 3; 24% and 4%, respectively, of the poses obtained) (Table 2). In NET-Cluster 2, fluoxetine is binding exclusively in the S1 site with the amine and unsubstituted phenyl ring located at similar positions as found in NET-Cluster 1, and in NET-Cluster 3 fluoxetine is binding in the S2 site in a similar pose as found in SERT-Cluster 3 (Fig. 2). NET-Cluster 1 and NET-Cluster 2 are not similar to any of the binding modes observed for fluoxetine within the S1 site of SERT.

Experimental validation of suggested binding modes of fluoxetine in SERT. To distinguish between the three obtained clusters of fluoxetine binding in SERT, we performed a mutational analysis of residues within 6 Å of the predicted binding modes to determine their role for fluoxetine potency. In total, 59 point-mutations across 27 different positions in the S1 and S2 sites of SERT were included in the study. Nine mutants rendered the transporter non-functional, and were not studied further (Supplemental Table 1). The inhibitory potency (K_i) of fluoxetine was determined at each of the 50 functional point-mutants across 24 different positions (Fig. 3 and Supplemental Table 1). At five positions (Tyr95, Asp98, Ile168, Ile172, Asn177), point-mutations induced >10-fold shift in the K_i-value for fluoxetine (ranging from 11- to 79-fold), suggesting these residues as key determinants for fluoxetine binding in SERT. As all five residues are all located within the S1 site of SERT, these results suggest SERT-Cluster 1 to represent the bioactive binding conformation of fluoxetine in SERT. This is in accordance with IFD calculations that also indicated fluoxetine to have the tightest binding in this cluster (Table 2), most significantly revealed in the Emodel-scores. In contrast, mutations of residues within the S2 site generally induced < 3-fold shift in fluoxetine K_i

Molecular Pharmacology Fast Forward. Published on February 10, 2014 as DOI: 10.1124/mol.113.091249
This article has not been copyedited and formatted. The final version may differ from this version.

(Fig. 3 and Supplemental Table 1), thus speaking against the binding modes predicted in SERT-Cluster 2 and SERT-Cluster 3. Notable, an ionic interaction between the amine of fluoxetine and the negatively charged side-chain of the S2 residue Glu493 on TM10 is predicted in the two minor binding clusters (Fig. 2a). However, removing the negatively charged side-chain by the E493A mutation had no significant effect on the potency of fluoxetine (Fig. 3 and Supplemental Table 1). Furthermore, mutations of six hydrophobic residues within the S2 site (Trp103, Ile179, Trp182, Tyr232, Val236 and Val489) that seems to be important for the overall shape of the extracellular vestibule of SERT, generally only led to small shifts (< 3-fold) in fluoxetine K_i (Fig. 3 and Supplemental Table 1), substantiating that SERT-Cluster 2 and SERT-Cluster 3 are not representing the bioactive binding conformation of fluoxetine in SERT. Interestingly, TM10 residues have previously been suggested to have an important role for inhibitor binding within the S1 site of *Drosophila* and human DAT (Bisgaard et al., 2011; Penmatsa et al., 2013). Here we show that mutation of residues in TM10 of SERT (Ala486, Val489, Lys490 and Glu493) induce < 3-fold changes in the potency of fluoxetine (Fig. 4 and Supplementary Table 1), suggesting that TM10 residues in DAT hold a more important role for inhibitor binding compared to TM10 residues in SERT. The amine of fluoxetine was found to have a key role for high-affinity binding in SERT (Table 1). According to SERT-Cluster 1, the amine forms a direct interactions with Tyr95 and Asp98 on TM1, similarly to what has previously been observed for escitalopram (Koldsø et al., 2010). Accordingly, the D98E mutation induced a 12-fold loss of potency for fluoxetine, and removal of the aromatic ring of Tyr95 (Y95A and Y95V) induced >40-fold loss of potency for fluoxetine (Fig. 3 and Supplemental Table 1). Interestingly, when substituting Tyr95 for Trp (Y95W) we found a significant 8-fold gain of potency (Fig. 3 and Supplemental Table 1). Since Trp is a better cation-π interaction partner compared to Tyr (Gallivan and Dougherty, 1999), the gain of potency induced by Y95W suggests a cation-π interaction between the amine of fluoxetine and the aromatic side-chain of Tyr95. The I168F mutation induced an 11-fold gain of potency for fluoxetine (Fig. 3 and Supplemental Table 1), which is likely induced by aromatic interactions between the inserted Phe and the unsubstituted phenyl ring of fluoxetine in the lower part of the S1 site (Figs. 2 and 3). Previously, the I172M mutation has been shown to decrease fluoxetine potency (Henry et al., 2006; Sørensen et al., 2012; Thompson et al., 2011; Walline et al., 2008). Here, we show that mutation of Ile172 to Ala, Gln and Met induced 6- to 79-fold loss of potency for fluoxetine and corroborate that Ile172 holds a key role for

Molecular Pharmacology Fast Forward. Published on February 10, 2014 as DOI: 10.1124/mol.113.091249
This article has not been copyedited and formatted. The final version may differ from this version.

recognition of fluoxetine (Fig. 3 and Supplemental Table 1). Mutation of Asn177 on TM3 to Ala or Ser induced 7- and 25-fold loss of potency for fluoxetine, respectively. In contrast, the N177E mutation did not significantly affect fluoxetine K_i (Fig. 3 and Supplemental Table 1), indicating that a side-chain bearing a carbonyl group in this position is important for recognition of fluoxetine. In SERT-Cluster 1, Asn177 is located > 6.5 Å away from fluoxetine but interacts with Thr439 through an H-bond (Fig. 3). Hence, the N177A and N177S mutations might affect fluoxetine K_i in an indirect manner by modulating the overall shape of the S1 pocket by disruption of the H-bond between TM3 and TM8. The CF_3 substituent of fluoxetine was found to be a key determinant for obtaining high affinity binding in SERT (Table 1). In SERT-Cluster 1, the CF_3-substituted phenyl ring is located in a hydrophobic pocket with a direct interaction between the CF_3 group and the backbone of Gly100 and aromatic π-π stacking interactions with Tyr176 (Fig. 3). Backbone interactions are notoriously difficult to address by conventional mutagenesis, and we have previously shown that SERT is very sensitive to mutation of Tyr176 (Andersen et al., 2010). Only the conservative Y176F mutation has so far been found to be functionally tolerated and had no significant effect on fluoxetine K_i (Fig. 3 and Supplemental Table 1). Therefore, as an alternative approach to probe specific interactions between the CF_3 substituted phenyl ring of fluoxetine and SERT, we tested nisoxetine, des-CF_3-fluoxetine (compound **8**) and 2-OCH_3-fluoxetine (compound **9**) at selected S1 mutations that induce significant changes in fluoxetine K_i (Supplemental Table 2). Nisoxetine, **8** and **9** have different aromatic substituents compared to fluoxetine, and we thus envisioned that if the substituted phenyl ring of fluoxetine interacts with one of the mutated residues, the analogs would be differentially affected by the mutation compared to fluoxetine. However, the potency of fluoxetine and the three analogs were generally affected to the same level across the tested mutations (Supplemental Table 2), thereby indirectly substantiating that the CF_3-substituted phenyl ring is located in the hydrophobic pocket, potentially engaging in backbone and aromatic stacking interactions that are difficult to address by site-directed mutagenesis. In summary, our mutational analysis establishes the S1 site as the primary binding site for fluoxetine in SERT and identifies SERT-Cluster 1 as the most likely binding mode model.

Molecular determinants for SERT/NET selectivity. We next sought to identify specific residues within SERT and NET that determines the distinct selectivity of fluoxetine and nisoxetine. We have shown that

Molecular Pharmacology Fast Forward. Published on February 10, 2014 as DOI: 10.1124/mol.113.091249
This article has not been copyedited and formatted. The final version may differ from this version.

non-conserved SERT/NET residues within the S1 site dictate the selectivity for citalopram (Andersen et al., 2011). Accordingly, we hypothesized that the molecular determinants for fluoxetine and nisoxetine selectivity is also found among these residues. We have previously mutated each of the 15 non-conserved SERT/NET residues found within 6 Å of the S1 site to the aligning residue in the other transporter, resulting in 15 individual SERT-to-NET mutations in SERT and 15 individual NET-to-SERT mutations in NET (Fig. 4 and Supplemental Figure 2) (Andersen et al., 2011). To systematically probe for the individual contribution of these non-conserved S1 residues for the selectivity of fluoxetine and nisoxetine, we determined the inhibitory potency of the two inhibitors at the 15 SERT-to-NET and at the 15 NET-to-SERT mutations (Fig. 4, Supplemental Table 3 and Supplemental Table 4). For six of the SERT-to-NET mutations in SERT, the potency of fluoxetine was significantly decreased (3- to 7-fold). None of the SERT mutants induced an increase in the potency of nisoxetine (Fig. 4 and Supplemental Table 3). In contrast, twelve of the 15 SERT-to-NET mutants in NET increased fluoxetine potency (3- to 11-fold), whereas only three mutants decreased the potency of nisoxetine (2- to 3-fold) (Fig. 4 and Supplemental Table 4). Hence, as observed for citalopram (Andersen et al., 2011), inhibitor selectivity can be modulated, but is not controlled by a single non-conserved residue within the S1 site. Next, we combined the single point-mutants into a set of 30 multiple SERT-to-NET mutants in SERT (designated S1-S30) and 17 multiple NET-to-SERT mutants in NET (designated N1-N17) (Fig. 4, Supplemental Table 3 and Supplemental Table 4). The design of these mutants was initially directed by results from single point mutants and later combined with results from multiple mutants and with the binding poses obtained from IFD calculations. Functional uptake activity was retained for 29 of the 30 multiple SERT mutants and for 10 of the 17 multiple NET mutants (Supplemental Table 3 and Supplemental Table 4). The non-functional mutants were not studied further. For fluoxetine, a significant loss of potency (3- to 11-fold) was observed for eight of the multiple SERT mutants (Fig. 5 and Supplemental Table 3). Mutations within the Ile172/Ala173/Ser174 motif on TM3 was included in the five multiple mutants that displayed the largest loss of potency, suggesting that this motif is an important determinant for the selectivity of fluoxetine. Interestingly, combining mutations in the Ile172/Ala172/Ser174 motif with A441G and L443M (as in S27, S28 and S29) induced a significant gain of potency for fluoxetine (Fig. 5 and Supplemental Table 3), indicating that A441G and L443M hold a positive role for binding of the SSRI. For nisoxetine, seven of the multiple SERT mutants induced a significant gain of potency (10- to 24-

Molecular Pharmacology Fast Forward. Published on February 10, 2014 as DOI: 10.1124/mol.113.091249
This article has not been copyedited and formatted. The final version may differ from this version.

fold). Combining mutations within the Ile172/Ala173/Ser174 motif with A441G and L443M on TM8 induced the largest gain of nisoxetine potency, indicating that residues on TM3 and TM8 are cooperative determinants for binding of nisoxetine in SERT. The three-fold S29 mutant (SERT-S174F-A441G-L443M) had the largest effect, and rendered SERT 24-fold more sensitive to nisoxetine compared to SERT WT (60 nM versus 1422 nM), showing that key determinants for nisoxetine selectivity are located within the S1 site of SERT.

Determination of the potency of nisoxetine at the ten functional multiple NET mutants surprisingly showed that all retained WT potency of the NET selective ligand (Fig. 4 and Supplemental Table 4). These data strongly suggest that, in contrast to SERT, non-conserved S1 residues do not define the inhibitory potency of nisoxetine in NET. In contrast, all multiple NET-to-SERT mutants induced a significant gain of fluoxetine potency (2- to 14-fold) (Fig. 5 and Supplemental Table 4). Mutations in TM1 (F72Y and A77G), TM8 (M424L and A426G) and TM9 (Thr453) were found to be most important for improving inhibitory potency of fluoxetine in NET. Specifically, the four-fold N9 mutant (NET-A77G-M424L-A426G-T453C) induced the largest effect and rendered NET 14-fold more sensitive towards fluoxetine compared to NET WT (2993 nM versus 217 nM). Hence, non-conserved residues within the S1 site of SERT and NET are key determinants for the selectivity of fluoxetine, which are supportive of our proposed binding mode of fluoxetine (Fig. 2).

Interchanging binding sites between SERT and NET. Interchanging non-conserved residues within the S1 site of SERT and NET modulated the potency of fluoxetine and nisoxetine. However, the selectivity was not fully reversed by any of the tested mutants. We therefore generated a series of mutant constructs in which all non-conserved residues in the S1 site and/or all non-conserved residues in the S2 site were simultaneously interchanged between SERT and NET, and thereby in principle transplanting these binding sites from SERT into NET and vice versa. Hereby, three SERT constructs containing NET S1 [SERT-(NET S1)], NET S2 [SERT-(NET S2)], and NET S1/S2 [SERT-(NET S1S2)], and two NET constructs containing SERT S1 [NET-(SERT S1)] and SERT S2 [NET-(SERT S2)] were created (Fig. 5, Supplemental Figure 2 and Supplemental Table 5). Additionally, we also created two constructs in which all non-conserved residues within 6 Å of the predicted binding mode of fluoxetine (SERT-Cluster 1) was interchanged [SERT-(NET

Molecular Pharmacology Fast Forward. Published on February 10, 2014 as DOI: 10.1124/mol.113.091249
This article has not been copyedited and formatted. The final version may differ from this version.

S1S2i) and NET-(SERT S1S2i), respectively] (for detailed description of mutant constructs, see Supplemental Figure 2 and Supplemental Table 5).

Initially, we performed saturation binding analysis on membrane preparations from COS7 cells expressing WT and mutant transporters and found that all SERT constructs bind [^{125}I]*β*-CIT, whereas only NET WT and NET-(SERT S2) showed specific [^{125}I]*β*-CIT binding (Fig. 5 and Supplemental Table 5). Consistent with saturation binding analyses, confocal imaging of GFP-tagged variants of WT and mutant transporters showed that the two NET constructs that do not bind [^{125}I]*β*-CIT, NET-(SERT S1) and NET-(SERT S1S2i), were primarily retained within intracellular compartments (Supplemental Figure 3). Next, we determined the binding affinities of fluoxetine and nisoxetine at the S1/S2 constructs that bind [^{125}I]*β*-CIT in a competition binding assay. For fluoxetine, insertion of NET S1 into SERT induced a 15-fold decrease in binding affinity (7 nM versus 102 nM), whereas insertion of the NET S2 site did not affect binding of fluoxetine (Fig. 5, Supplemental Table 5). Interestingly, the decreased binding affinity of fluoxetine in SERT-(NET S1) was reversed by simultaneous insertion of S2 site (Fig. 5 and Supplemental Table 5). The binding affinity of nisoxetine was increased by 6-fold when inserting the S1 site from NET into SERT (167 nM versus 29 nM), whereas insertion of the S2 site had no significant effect on nisoxetine. Insertion of both the S1 and S2 sites from NET into SERT improved the binding affinity of nisoxetine to a similar level as observed when the S1 site was inserted alone (15 nM versus 29 nM), showing that residues located in the S1 site of SERT are key determinants for the selectivity of nisoxetine.

Similar detailed analysis was not possible for NET, since only the NET-(SERT S2) construct could bind [^{125}I]*β*-CIT. Interestingly, the binding affinity of nisoxetine was decreased almost to the same level as observed in SERT WT by inserting SERT S2 into NET (167 nM versus 104 nM compared to 4 nM at NET WT). Together with our initial analysis, that showed non-conserved S1 residues in NET to have a minor role for the selectivity of nisoxetine, this result emphasize that non-conserved residues in the S2 site of NET are key determinants for the selectivity of nisoxetine. In summary, our mutational analysis of non-conserved SERT/NET residues supports that the selectivity of fluoxetine for SERT over NET is largely determined by non-conserved residues within the S1 site of both SERT and NET, which is fully in accordance with our proposed IFD models of fluoxetine binding within the S1 site in the two transporters. In contrast, we found

Molecular Pharmacology Fast Forward. Published on February 10, 2014 as DOI: 10.1124/mol.113.091249
This article has not been copyedited and formatted. The final version may differ from this version.

that the selectivity of nisoxetine for NET over SERT is controlled by non-conserved residues in different regions of SERT (S1 residues) and NET (S2 residues). Differentiation between direct and indirect effects in mutagenesis studies is inherently difficult. Mutations can induce long range allosteric effects that perturb a distinct binding site or induce a shift in the conformational equilibrium of the transporter that changes the temporal accessibility to the binding site. Thus, the mutational analyses do not allow us to conclude on the location of the nisoxetine binding site in SERT and NET, but emphasize that there is a complex mechanism for selective recognition of inhibitors in SERT and NET.

DISCUSSION

The models of fluoxetine binding in human SERT and NET that are produced in the present study are based on X-ray crystal structures of LeuT and have been constructed using well-established procedures that have been implemented for modeling of other important monoamine transporter inhibitors (Andersen et al., 2010; Koldsø et al., 2010; Severinsen et al., 2013; Sinning et al., 2010). Very recently, *Drosophila* DAT and LeuBAT were crystallized in complex with antidepressants (Penmatsa et al., 2013; Wang et al., 2013). These X-ray crystal structures offer a new platform for understanding ligand interactions that have obvious potential to further push the field toward more reliable and realistic models of antidepressant binding in human transporters. However, both *Drosophila* DAT and LeuBAT are inactive in transport and their pharmacological profiles seem to be a hybrid of the human SERT, NET and DAT. Thus, in order to assess the potential of LeuBAT and *Drosophila* DAT for studying the molecular pharmacology of human transporters, it is critically important to establish similarities and discrepancies between *Drosophila* DAT and LeuBAT and their human relatives. For this purpose, comparison of our present fluoxetine model with the X-ray crystal structure of LeuBAT in complex with fluoxetine therefore provides an excellent first opportunity for assessment of the potential of LeuBAT as a model system for SSRI binding in human transporters. First and foremost, our proposed binding model of fluoxetine in SERT (SERT-Cluster 1) is in agreement with the LeuBAT structure (Wang et al., 2013) by showing that the inhibitor bind within the S1 site (Fig. 2 and Fig. 3). The observed S1 binding modes in LeuBAT and our SERT model correlate very well

Molecular Pharmacology Fast Forward. Published on February 10, 2014 as DOI: 10.1124/mol.113.091249
This article has not been copyedited and formatted. The final version may differ from this version.

with our experimental validation, and can explain two key findings from the mutational analysis. Firstly, fluoxetine potency is largely affected by mutations in the S1 site (up to 79-fold loss-of-potency), whereas mutations in the S2 site generally induce < 3-fold changes in fluoxetine K_i (Fig. 3 and Supplemental Table 1). Secondly, our mutational analysis suggest a cation-π interaction between Tyr95 and the amino group of fluoxetine, which is in agreement with our binding model showing that the amino group of fluoxetine is anchored between Tyr95 and Asp98 in the S1 site of SERT. A similar interaction is also observed in LeuBAT, where the amino group of fluoxetine is coordinated by the aligning residues (Tyr21 and Asp24, respectively) within the S1 site (Wang et al., 2013). Together with experimentally validated models showing other SERT inhibitors to also be anchored within the S1 site (Andersen et al., 2010; Combs et al., 2011; Koldsø et al., 2010; Severinsen et al., 2013; Sinning et al., 2010), this is in contrast to previous structural studies of LeuT in complex with antidepressants, that propose SSRIs and TCAs to bind in the S2 site (Zhou et al., 2007; Zhou et al., 2009). Hence, although crystal structures of LeuT have provided seminal improvements for our understanding of the overall structure and function of SERT and NET, our results emphasize that LeuBAT is an improved model system compared to LeuT for understanding the mechanism of drug binding in human transporters.

However, we do observe differences between fluoxetine binding in our model compared to the LeuBAT structure. Specifically, although the amine of fluoxetine is anchored similarly between the Tyr and Asp residues, the orientation of the two aromatic moieties of the inhibitor is reversed in our model compared to the LeuBAT structure (Fig. 6). While the CF_3-substituted phenyl ring binds between TM3 and TM8 in the LeuBAT structure, it is protruding up towards the S2 site in our model. Notably, neither from IFDs in SERT nor in NET did we identify any poses of fluoxetine in an orientation similar to the one in the LeuBAT structure (Fig. 2). Furthermore, observations from our mutational analysis of SERT are difficult to reconcile with the orientation of the two aromatic moieties of fluoxetine as found in LeuBAT. Specifically, the CF_3-group of fluoxetine is sandwiched in a groove between TM3 and TM8 in LeuBAT (Wang et al., 2013). In contrast, in our SERT model we observed an H-bond between the carbonyl group on the Asn177 side-chain and the hydroxyl group of the Thr439 side-chain, which is not conserved in LeuBAT. This H-bond constrains flexibility of TM3 and TM8 and does not allow a similar binding mode of the CF_3-group of

Molecular Pharmacology Fast Forward. Published on February 10, 2014 as DOI: 10.1124/mol.113.091249
This article has not been copyedited and formatted. The final version may differ from this version.

fluoxetine in SERT (Fig. 6). Accordingly, we found that mutation of Asn177 and Thr439 induce a marked loss-of-potency for fluoxetine (Fig. 3 and Fig. 4), likely due to disruption of the H-bond and thereby the overall shape of the binding site rather than affecting direct interactions with the inhibitor. Also, if fluoxetine adopts the same binding mode in SERT as found in LeuBAT, Asn177 would be pointing directly towards the CF_3-group of the SSRI (Fig. 6). Thus, introduction of a negative charge into this sub-site would likely cause an electrostatic repulsion with the electronegative CF_3-group, and thereby induce a loss-of-potency for fluoxetine. Notably, the N177E mutation had no effect on fluoxetine potency (Fig. 3), and since the H-bond to Thr439 can be preserved in the N177E mutant, this provides further support for our proposed binding model. Additionally, mutation of Ile179 in SERT has previously been shown to induce a marked loss-of-potency for fluoxetine (Zhou et al., 2009). This is in good agreement with our binding model, in which Ile179 is located within 3.5Å from fluoxetine and points directly towards the sub-site where the CF_3 group of fluoxetine binds (Fig. 6). In contrast, if fluoxetine adopts a similar binding mode in SERT as found in LeuBAT, Ile179 would be located > 6.5Å away from the inhibitor (Fig. 6), making it less likely that mutation at this site will have a pronounced effect on fluoxetine potency. Overall, even though fluoxetine share the same binding site in human SERT and LeuBAT, our experimentally supported binding model of fluoxetine in SERT suggest that the SSRI has distinct binding modes in human and bacterial transporters, emphasizing the continued need for careful experimental validation when extrapolating findings from LeuBAT to human transporters.

Our study provides novel insight into the molecular determinants for selective nisoxetine binding in NET by showing that non-conserved residues within the S2 site are important for high-affinity nisoxetine binding in NET (Fig. 4 and Fig. 5). Mutation of residues outside the S1 site in NET has previously been found to affect binding of nisoxetine (Paczkowski et al., 2007; Wenge and Bönisch, 2013). In addition, cocaine-like compounds, which are believed to bind in the S1 site of monoamine transporters (Beuming et al., 2008), display non-competitive binding with nisoxetine in NET (Zhen et al., 2012). Together, these observations indicate that nisoxetine bind outside the S1 site, and are thus supportive of a recent model suggesting that nisoxetine binds to the S2 site in NET (Wang et al., 2012). However, nisoxetine is also affected by mutations of S1 residues in NET (Mason et al., 2007; Sørensen et al., 2012), and the recent structures of *Drosophila*

Molecular Pharmacology Fast Forward. Published on February 10, 2014 as DOI: 10.1124/mol.113.091249
This article has not been copyedited and formatted. The final version may differ from this version.

DAT and LeuBAT showed a common inhibitor binding site to be located within the central S1 site (Penmatsa et al., 2013; Wang et al., 2013). Taken together, it seems most likely that the high-affinity binding site for nisoxetine is located within the S1 site in NET, and that the selectivity is determined by non-conserved residues lining the S2 site that nisoxetine needs to permeate in order to reach the central S1 site. In contrast, we find that the molecular determinants that underlie the lower potency of nisoxetine in SERT are primarily located among non-conserved residues within the S1 site of this transporter (Fig. 4 and Fig. 5). This is in agreement with previous findings of other S1 residues in SERT that have been shown to be important for recognition of nisoxetine in SERT (Sørensen et al., 2012; Walline et al., 2008). Hence, in contrast to fluoxetine where S1 residues in both SERT and NET control binding and selectivity (Fig. 3 and Fig. 4), selective binding of nisoxetine is controlled by residues in separate regions of the two transporters. Interestingly, the same pattern has also been found for the SSRI escitalopram and the structurally closely related NET selective inhibitor talopram (Andersen et al., 2011). Thus, the finding that the selectivity of seemingly closely related inhibitors are controlled by residues located in different regions of two closely related transporters suggest a complexity of the molecular pharmacology of monoamine transporters that warrant further studies.

In summary, our findings add important new information on the molecular basis for SERT/NET selectivity of antidepressants and provide the first assessment of the potential of LeuBAT as model system for antidepressant binding to human transporters. Along with a growing number of other LeuT derived models of inhibitor binding, we can now begin to understand the differences and similarities among the inhibitory mechanisms of antidepressants in a structural context. This is essential for establishing a useful framework for structure-based drug development of future monoamine transporter drugs with fine-tuned transporter selectivity.

Molecular Pharmacology Fast Forward. Published on February 10, 2014 as DOI: 10.1124/mol.113.091249
This article has not been copyedited and formatted. The final version may differ from this version.

ACKNOWLEDGEMENTS

We thank Mr. Shahrokh Padrah for technical assistance with synthesis of fluoxetine analogues and Ms. B. Kegel for performing elemental analysis of the synthesized compounds.

AUTHORSHIP CONTRIBUTIONS

Participated in research design: Andersen, Koldsø, Schiøtt, Strømgaard, Kristensen

Conducted experiments: Andersen, Stuhr-Hansen, Zachariassen, Koldsø

Performed data analysis: Andersen, Koldsø, Schiøtt, Strømgaard, Kristensen

Wrote or contributed to the writing of the manuscript: Andersen, Koldsø, Schiøtt, Strømgaard, Kristensen

REFERENCES

Andersen J, Olsen L, Hansen KB, Taboureau O, Jørgensen FS, Jørgensen AM, Bang-Andersen B, Egebjerg J, Strømgaard K and Kristensen AS (2010) Mutational mapping and modeling of the binding site for (S)-citalopram in the human serotonin transporter. *J Biol Chem* **285**(3): 2051-2063.

Andersen J, Stuhr-Hansen N, Zachariassen L, Toubro S, Hansen SMR, Eildal JNN, Bond AD, Bøgesø KP, Bang-Andersen B, Kristensen AS and Strømgaard K (2011) Molecular determinants for selective recognition of antidepressants in the human serotonin and norepinephrine transporters. *Proc Natl Acad Sci USA* **108**(29): 12137-12142.

Andersen J, Taboureau O, Hansen KB, Olsen L, Egebjerg J, Strømgaard K and Kristensen AS (2009) Location of the Antidepressant Binding Site in the Serotonin Transporter: Importance of Ser-438 in Recognition of Citalopram and Tricyclic Antidepressants. *J Biol Chem* **284**(15): 10276-10284.

Apparsundaram S, Stockdale DJ, Henningsen RA, Milla ME and Martin RS (2008) Antidepressants targeting the serotonin reuptake transporter act via a competitive mechanism. *J Pharmacol Exp Ther* **327**: 982-990.

Barker EL, Moore KR, Rakhshan F and Blakely RD (1999) Transmembrane domain I contributes to the permeation pathway for serotonin and ions in the serotonin transporter. *J Neurosci* **19**(12): 4705-4717.

Bauer M, Monz BU, Montejo AL, Quail D, Dantchev N, Dernyttenaere K, Garcia-Cebrian A, Grassi L, Perahia DGS, Reed C and Tylee A (2008) Prescribing patterns of antidepressants in europe: Results from the Factors Influencing Depression Endpoints Research (FINDER) study. *Eur Psychiatry* **23**(1): 66-73.

Beuming T, Kniazeff J, Bergmann ML, Shi L, Gracia L, Raniszewska K, Newman AH, Javitch JA, Weinstein H, Gether U and Loland CJ (2008) The binding sites for cocaine and dopamine in the dopamine transporter overlap. *Nat Neurosci* **11**(7): 780-789.

Bisgaard H, Larsen MAB, Mazier S, Beuming T, Newman AH, Weinstein H, Shi L, Loland CJ and Gether U (2011) The binding sites for benztropines and dopamine in the dopamine transporter overlap. *Neuropharmacology* **60**(1): 182-190.

Celik L, Sinning S, Severinsen K, Hansen CG, Møller MS, Bols M, Wiborg O and Schiøtt B (2008) Binding of serotonin to the human serotonin transporter. Molecular modeling and experimental validation. *J Am Chem Soc* **130**(12): 3853-3865.

Combs S, Kaufmann K, Field JR, Bakely RD and Meiler J (2011) Y95 and E444 Interaction Required for High-Affinity S-Citalopram Binding in the Human Serotonin Transporter. *ACS Chem Neurosci* **2**(2): 75-81.

Friesner RA, Banks JL, Murphy RB, Halgren TA, Klicic JJ, Mainz DT, Repasky MP, Knoll EH, Shelley M, Perry JK, Shaw DE, Francis P and Shenkin PS (2004) Glide: a new approach for rapid, accurate docking and scoring. 1. Method and assessment of docking accuracy. *J Med Chem* **47**(7): 1739-1749.

Gallivan JP and Dougherty DA (1999) Cation-pi interactions in structural biology. *Proc Natl Acad Sci USA* **96**(17): 9459-9464.

Graham D, Esnaud H, Habert E and Langer SZ (1989) A common binding site for tricyclic and nontricyclic 5-hydroxytryptamine uptake inhibitors at the substrate recognition site of the neuronal sodium-dependent 5-hydroxytryptamine transporter. *Biochem Pharmacol* **38**(21): 3819-3826.

Henry LK, Field JR, Adkins EM, Parnas ML, Vaughan RA, Zou MF, Newman AH and Blakely RD (2006) Tyr-95 and Ile-172 in transmembrane segments 1 and 3 of human serotonin transporters interact to establish high affinity recognition of antidepressants. *J Biol Chem* **281**(4): 2012-2023.

Horng JS and Wong DT (1976) Effects of serotonin uptake inhibitor, Lilly 110140, on transport of serotonin in rat and human blood platelets. *Biochem Pharmacol* **25**(7): 865-867.

Kaufmann KW, Dawson ES, Henry LK, Field JR, Blakely RD and Meiler J (2009) Structural determinants of species-selective substrate recognition in human and Drosophila serotonin transporters revealed through computational docking studies. *Proteins* **74**(3): 630-642.

Koe BK, Lebel LA and Welch WM (1990) [^{3}H]-Sertraline Binding to Rat Brain Membranes. *Psychopharmacology* **100**(4): 470-476.

Koldsø H, Autzen HE, Grouleff J and Schiøtt B (2013a) Ligand Induced Conformational Changes of the Human Serotonin Transporter Revealed by Molecular Dynamics Simulations. *Plos One* **8**(6): e63635.

Koldsø H, Christiansen AB, Sinning S and Schiøtt B (2013b) Comparative Modeling of the Human Monoamine Transporters: Similarities in Substrate Binding. *ACS Chem Neurosci* **4**(2): 295-309.

Koldsø H, Severinsen K, Tran TT, Celik L, Jensen HH, Wiborg O, Schiøtt B and Sinning S (2010) The Two Enantiomers of Citalopram Bind to the Human Serotonin Transporter in Reversed Orientations. *J Am Chem Soc* **132**(4): 1311-1322.

Krishnamurthy H and Gouaux E (2012) X-ray structures of LeuT in substrate-free outward-open and apo inward-open states. *Nature* **481**(7382): 469-474.

Kristensen AS, Andersen J, Jørgensen TN, Sørensen L, Eriksen J, Loland CJ, Strømgaard K and Gether U (2011) The *SLC6* neurotransmitter transporters: structure, function and regulation *Pharmcol Rev* **63**: 585-640.

Kristensen AS, Larsen MB, Johnsen LB and Wiborg O (2004) Mutational scanning of the human serotonin transporter reveals fast translocating serotonin transporter mutants. *Eur J Neurosci* **19**(6): 1513-1523.

Mason JN, Deecher DC, Richmond RL, Stack G, Mahaney PE, Trybulski E, Winneker RC and Blakely RD (2007) Desvenlafaxine succinate identifies novel antagonist binding determinants in the human norepinephrine transporter. *J Pharmacol Exp Ther* **323**(2): 720-729.

Owens MJ, Morgan WN, Plott SJ and Nemeroff CB (1997) Neurotransmitter receptor and transporter binding profile of antidepressants and their metabolites. *J Pharmacol Exp Ther* **283**(3): 1305-1322.

Paczkowski FA, Sharpe IA, Dutertre S and Lewis RJ (2007) χ-conotoxin and tricyclic antidepressant interactions at the norepinephrine transporter define a new transporter model. *J Biol Chem* **282**(24): 17837-17844.

Penmatsa A, Wang KH and Gouaux E (2013) X-ray structure of dopamine transporter elucidates antidepressant mechanism. *Nature* **503**(7474): 85-90.

Plenge P, Shi L, Beuming T, Te J, Newman AH, Weinstein H, Gether U and Loland CJ (2012) Steric hindrance mutagenesis in the conserved extracellular vestibule impedes allosteric binding of antidepressants to the serotonin transporter. *J Biol Chem* **287**(47): 39316-39326.

Schrödinger Suite 2011 Induced Fit Docking protocol, Glide version 5.7, Schrödinger, LLC, New York, NY, 2011 and Prime version 3.0, Schrödinger LLC New York, NY, 2011.

Severinsen K, Koldsø H, Thorup KA, Schjøth-Eskesen C, Møller PT, Wiborg O, Jensen HH, Sinning S and Schiøtt B (2013) Binding of Mazindol and Analogs to the human Serotonin and Dopamine Transporters. *Mol Pharmacol*: in press.

Severinsen K, Kraft JF, Koldsø H, Vinberg KA, Rothman RB, Partilla JS, Wiborg O, Blough B, Schiøtt B and Sinning S (2012) Binding of the Amphetamine-like 1-Phenyl-piperazine to Monoamine Transporters. *ACS Chem Neurosci* **3**(9): 693-705.

Sherman W, Day T, Jacobson MP, Friesner RA and Farid R (2006) Novel procedure for modeling ligand/receptor induced fit effects. *J Med Chem* **49**(2): 534-553.

Singh SK, Yamashita A and Gouaux E (2007) Antidepressant binding site in a bacterial homologue of neurotransmitter transporters. *Nature* **448**(7156): 952-956.

Sinning S, Musgaard M, Jensen M, Severinsen K, Celik L, Koldsø H, Meyer T, Bols M, Jensen HH, Schiøtt B and Wiborg O (2010) Binding and orientation of tricyclic antidepressants within the central substrate site of the human serotonin transporter. *J Biol Chem* **285**(11): 8363-8374.

Sørensen L, Andersen J, Thomsen M, Hansen SMR, Zhao XB, Sandelin A, Strømgaard K and Kristensen AS (2012) Interaction of Antidepressants with the Serotonin and Norepinephrine Transporters: Mutational studies of the S1 substrate binding pocket. *J Biol Chem* **287**(52): 43694-43707.

Tavoulari S, Forrest LR and Rudnick G (2009) Fluoxetine (Prozac) binding to serotonin transporter is modulated by chloride and conformational changes. *J Neurosci* **29**(30): 9635-9643.

Thompson BJ, Jessen T, Henry LK, Field JR, Gamble KL, Gresch PJ, Carneiro AM, Horton RE, Chisnell PJ, Belova Y, McMahon DG, Daws LC and Blakely RD (2011) Transgenic elimination of high-affinity antidepressant and cocaine sensitivity in the presynaptic serotonin transporter. *Proc Natl Acad Sci USA* **108**(9): 3785-3790.

Waitekus AB and Kirkpatrick P (2004) Duloxetine hydrochloride. *Nat Rev Drug Discov* **3**(11): 907-908.

Walline CC, Nichols DE, Carroll FI and Barker EL (2008) Comparative molecular field analysis using selectivity fields reveals residues in the third transmembrane helix of the serotonin transporter associated with substrate and antagonist recognition. *J Pharmacol Exp Ther* **325**(3): 791-800.

Wang CIA, Shaikh NH, Ramu S and Lewis RJ (2012) A Second Extracellular Site Is Required for Norepinephrine Transport by the Human Norepinephrine Transporter. *Mol Pharmacol* **82**(5): 898-909.

Wang H, Goehring A, Wang KH, Penmatsa A, Ressler R and Gouaux E (2013) Structural basis for action by diverse antidepressants on biogenic amine transporters. *Nature* **503**(7474): 141-145.

Wenge B and Bönisch H (2013) The role of cysteines and histidins of the norepinephrine transporter. *Neurochem Res* **38**(7): 1303-1314.

Wong DT, Bymaster FP and Engleman EA (1995) Prozac (Fluoxetine, Lilly-110140), the First Selective Serotonin Uptake Inhibitor and an Antidepressant Drug - 20 Years since Its First Publication. *Life Sci* **57**(5): 411-441.

Wong DT, Bymaster FP, Horng JS and Molloy BB (1975) New selective inhibitor for uptake of serotonin into synaptosomes of rat-brain - 3-(para-trifluoromethylphenoxy)-*N*-methyl-3-phenylpropylamine. *J Pharmacol Exp Ther* **193**(3): 804-811.

Wong DT, Bymaster FP, Reid LR, Fuller RW and Perry KW (1985) Inhibition of serotonin uptake by optical isomers of fluoxetine. *Drug Devel Res* **6**(4): 397-403.

Wong DT, Perry KW and Bymaster FP (2005) The discovery of fluoxetine hydrochloride (Prozac). *Nat Rev Drug Discov* **4**(9): 764-774.

Yamashita A, Singh SK, Kawate T, Jin Y and Gouaux E (2005) Crystal structure of a bacterial homologue of Na^+/Cl^--dependent neurotransmitter transporters. *Nature* **437**(7056): 215-223.

Zhen J, Ali S, Dutta AK and Reith ME (2012) Characterization of [^{3}H]CFT binding to the norepinephrine transporter suggests that binding of CFT and nisoxetine is not mutually exclusive. *J Neurosci Methods* **203**(1): 19-27.

Zhou Z, Zhen J, Karpowich NK, Goetz RM, Law CJ, Reith MEA and Wang DN (2007) LeuT-desipramine structure reveals how antidepressants block neurotransmitter reuptake. *Science* **317**(5843): 1390-1393.

Zhou Z, Zhen J, Karpowich NK, Law CJ, Reith MEA and Wang DN (2009) Antidepressant specificity of serotonin transporter suggested by three LeuT-SSRI structures. *Nat Struct Mol Biol* **16**(6): 652-657.

Molecular Pharmacology Fast Forward. Published on February 10, 2014 as DOI: 10.1124/mol.113.091249
This article has not been copyedited and formatted. The final version may differ from this version.

FOOTNOTES

The Lundbeck Foundation, the Danish National Research Foundation (DNRF59) and the Danish Council for Independent Research, Natural Sciences (FNU) are acknowledged for financial support.

Reprints requests to: Jacob Andersen, Department of Drug Design and Pharmacology, University of Copenhagen, Universitetsparken 2, DK-2100 Copenhagen, Denmark. E-mail: jaa@sund.ku.dk.

Current address for Heidi Koldsø: Department of Biochemistry, University of Oxford, South Parks Road, Oxford OX1 3QU, United Kingdom.

Molecular Pharmacology Fast Forward. Published on February 10, 2014 as DOI: 10.1124/mol.113.091249
This article has not been copyedited and formatted. The final version may differ from this version.

FIGURE LEGENDS

Figure 1. (**A**, **B**) Chemical structure and pharmacological characterization of the SSRI fluoxetine (**A**) and the NET selective congener nisoxetine (**B**). The binding affinities of fluoxetine and nisoxetine towards SERT (filled grey circles) and NET (filled blue circles) was determined in a [^{125}I]β-CIT competition binding assay. Data points represent mean ± S.E.M from triplicate determinations. (**C**) *Left;* Cross-sectional illustration of crystal structure of LeuT in complex with the substrate leucine (C-atoms shown in yellow) in the central S1 site and fluoxetine (FLX; C-atoms shown in green) in the vestibular S2 site (PDB ID 3GWW). *Right;* Cross-sectional illustration of crystal structure of LeuBAT in complex with fluoxetine (FLX; C-atoms shown in green) in the central S1 site (PDB ID 4MM8).

Figure 2. (**A**, **B**) Global binding clusters obtained from IFD simulations of *R*-fluoxetine (C-atoms shown in yellow) and *S*-fluoxetine (C-atoms shown in orange) into homology models of SERT (**a**) and NET (**b**). The two dominating binding clusters (SERT-Cluster 1 and NET-Cluster 1) represent 89% and 67% of all *R*- and *S*-fluoxetine poses obtained from IFD simulations into SERT and NET, respectively (Table 2). Note that the *R*- and *S*-enantiomers are completely overlapping in the two dominating binding clusters, whereas only a single enantiomer are found in the minor binding clusters (SERT-Cluster 2-3 and NET-Cluster 2-3). Selected residues in proximity of the proposed binding clusters are shown as stick representations, and the sodium ions are shown as magenta spheres. The stippled lines indicate the curvature of the S1 and S2 sites.

Figure 3. (**A**) Graphical summary of the fold-change in fluoxetine potency (shown on x-axis) induced by point-mutations at various positions in the S1 and S2 sites and in the S1/S2 interface (shown on y-axis). The fold-change is calculated as K_i(WT SERT)/K_i(mutant) or K_i(mutant)/K_i(WT SERT) for mutations increasing or decreasing the potency of fluoxetine, respectively. The grey shaded region indicate <10-fold change in fluoxetine potency. Open circles specifies that the mutation do not significantly affect the K_i-value for fluoxetine compared to WT SERT, whereas grey and blue shading of data points specify a significant change ($p < 0.01$; Student's *t*-test). Mutations producing >10-fold change in K_i and their corresponding positions are

Molecular Pharmacology Fast Forward. Published on February 10, 2014 as DOI: 10.1124/mol.113.091249
This article has not been copyedited and formatted. The final version may differ from this version.

highlighted in blue. Fluoxetine K_i, substrate K_m and functional activity of the mutations are shown in Supplemental Table 1. (**B**-**E**) Close-up views of a representative binding pose of *S*-fluoxetine (C-atoms shown in orange) in SERT from the dominating SERT-Cluster 1. Selected binding site residues are shown as stick representation. Positions where mutation induced >10-fold change in fluoxetine K_i are highlighted in blue. Sodium and chloride ions are shown as magenta and green spheres, respectively.

Figure 4. (**A**, **B**) Topology diagram of SERT (**A**) and NET (**B**) illustrating the identity, TM location and numbering of the 15 non-conserved SERT/NET residues within 6Å of the putative S1 site, and a graphical representation of selected multiple SERT and NET mutants (see also Supplemental Figure 1, Supplemental Table 3 and Supplemental Table 4). SERT mutants are shown on a grey background with mutations indicated in blue (**A**) and NET mutants are shown on a blue background with mutations indicated in grey (**B**)**.** (**C**-**F**) Inhibitory potency of fluoxetine and nisxoetine at single point-mutants in SERT (**C**) and NET (**D**) and at multiple mutants in SERT (**E**) and NET (**F**). The inhibitory potency of fluoxetine and nisoxetine was determined in a functional uptake inhibition assay, and data represent mean ± S.E.M. from at least three independent experiments each performed in triplicate (Supplemental Table 3 and Supplemental Table 4). The stippled lines indicate the potency of the inhibitors at WT transporters. *Asteriks* denote significantly different K_i value compared with WT transporters ($p < 0.01$; Student's *t*-test).

Figure 5. (**A**) Location of non-conserved SERT/NET residues within 6Å of the S1 site (*left*), S2 site (*middle*) and the putative fluoxetine binding site (*right*) shown on a homology model of SERT (see Supplemental Figure 2 and Supplemental Table 5 for specific residues). (**B**) Saturation binding curves for [^{125}I]β-CIT binding to COS-7 membranes expressing WT and mutant forms of SERT (*left*) and NET (*right*) where all non-conserved residues within 6Å of putative binding regions have been interchanged (for K_d and B_{max} values, see Supplemental Table 5). Data points represent mean ± S.E.M from duplicate determinations. (**C**, **D**) The binding affinities of fluoxetine and nisoxetine were determined in a [^{125}I]β-CIT competition binding assay at WT and mutant forms of SERT (**C**) and NET (**D**), and data represent mean ± S.E.M. from at least

Molecular Pharmacology Fast Forward. Published on February 10, 2014 as DOI: 10.1124/mol.113.091249
This article has not been copyedited and formatted. The final version may differ from this version.

three independent experiments each performed in duplicate (Supplemental Table 5). The stippled lines indicate the binding affinities of fluoxetine and nisoxetine at WT transporters.

Figure 6. (**A**, **B**) Superimposition of a representative binding pose of fluoxetine (C-atoms shown in orange) in SERT from the dominating SERT-Cluster 1 (same binding pose as shown in Fig. 2b-e) and the binding mode of fluoxetine (C-atoms shown in green) in LeuT (PDB ID 3GWW) (**A**) and fluoxetine (C-atoms shown in magenta) in LeuBAT (**B**). The overlays are shown on SERT model. Selected residues in proximity of the proposed binding clusters are shown as stick representations. Positions where mutation induce >10-fold change in fluoxetine potency is highlighted in dark blue. (**C**) Superimposition of a representative binding pose of fluoxetine (C-atoms shown in orange) in SERT (shown in grey) and the binding mode of fluoxetine (C-atoms shown in magenta) in LeuBAT (shown in blue). Selected residues in proximity of the proposed binding clusters are shown as stick representations. Numbering and identity of LeuBAT residues are shown in brackets. H-bond between SERT residues Asn177 and Thr439 is indicated by stippled line.

Molecular Pharmacology Fast Forward. Published on February 10, 2014 as DOI: 10.1124/mol.113.091249
This article has not been copyedited and formatted. The final version may differ from this version.

TABLES

Table 1.

Binding affinity of fluoxetine and nisoxetine derivatives at SERT and NET.

The binding affinities at human SERT and NET were determined in a [^{125}I]*β*-CIT competition binding assay, and the selectivity ratio was calculated as K_i(NET WT)/K_i(SERT WT).

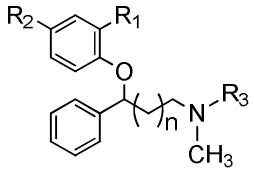

Compound	R_1	R_2	R_3	n	SERT WT (nM)	NET WT (nM)	SERT/NET selectivity
Fluoxetine (**1**)					7 ± 2	887 ± 115	127
S-Fluoxetine (*S*-**1**)	H	CF_3	H	1	3 ± 1	1,324 ± 246	389
R-Fluoxetine (*R*-**1**)					5 ± 1	572 ± 67	108
Nisoxetine (**2**)	OCH_3	H	H	1	167 ± 31	4 ± 1	0.02
N-Methylfluoxetine (**7**)	H	CF_3	CH_3	1	37 ± 4	10,563 ± 1,131	286
Des-CF_3-fluoxetine (**8**)	H	H	H	1	157 ± 29	12 ± 2	0.08
2-OCH_3-fluoxetine (**9**)	OCH_3	CF_3	H	1	3 ± 1	125 ± 22	45
Homofluoxetine (**10**)	H	CF_3	H	2	12 ± 1	3,352 ± 593	279
N-Methylhomofluoxetine (**11**)	H	CF_3	CH_3	2	992 ± 34	7,958 ± 1,196	8

Molecular Pharmacology Fast Forward. Published on February 10, 2014 as DOI: 10.1124/mol.113.091249
This article has not been copyedited and formatted. The final version may differ from this version.

Table 2.

Results from SERT and NET docking calculations.

The IFD setup is mentioned (either Small or Large). It is indicated if the cluster is located within the S1 or S2 site in addition to the cluster name for that setup. The number of poses in each cluster is listed with respect to the total number of poses. The average XP Gscore is listed with the standard deviation indicated in brackets. Also, the average Emodel score is listed with the standard deviation in brackets, and last it is listed in which global cluster the setup cluster belongs to.

Protein	IFD	Compound	S1 or S2 site	Cluster	#pose/ #total poses	Avg. XP GScore (kcal/mol)	Avg. Emodel (kcal/mol)	Global Cluster
hSERT	Small	R-Fluoxetine	S1	**S1-C1**	20/20	-11.7 [0.5]	-74.0 [9.5]	**SERT-Cluster 1**
				Outliers	0/20			
		S-Fluoxetine	S1	**S1-C1**	19/19	-11.5 [0.7]	-71.0 [8.1]	**SERT-Cluster 1**
				Outliers	0/19			
	Large	R-Fluoxetine	S2	**S2-C1**	4/4	-11.0 [0.4]	-65.2 [3.2]	**SERT-Cluster 2**
				Outliers	0/4			
		S-Fluoxetine	S1	**S1-C1**	1/2	-12.3 [-]	-81.4 [-]	**SERT-Cluster 1**
			S2	**S2-C1**	1/2	-11.0 [-]	-61.8 [-]	**SERT-Cluster 3**
				Outliers	0/2			
hNET	Small	R-Fluoxetine	S1	**S1-C1**	16/17	-10.6 [1.3]	-69.8 [5.8]	**NET-Cluster 1**
				Outliers	1/17			
		S-Fluoxetine	S1	**S1-C1**	12/19	-11.4 [0.6]	-69.1 [5.0]	**NET-Cluster 1**
			S1	**S1-C2**	6/19	-9.9 [0.3]	-55.3 [5.6]	**NET-Cluster 2**
				Outliers	1/19			
	Large	R-Fluoxetine	S1	**S1-C2**	2/5	-10.6 [0.5]	-53.0 [5.8]	**NET-Cluster 2**
			S2	**S2-C1**	2/5	-10.9 [0.2]	-66.8 [1.8]	**NET-Cluster 3**
				Outliers	1/5			
		S-Fluoxetine	S1	**S1-C1**	3/8	-11.7 [0.0]	-74.8 [0.7]	**NET-Cluster 1**
			S1	**S1-C2**	4/8	-10.0 [0.2]	-57.0 [2.4]	**NET-Cluster 2**
				Outliers	1/8			

Figure 1.

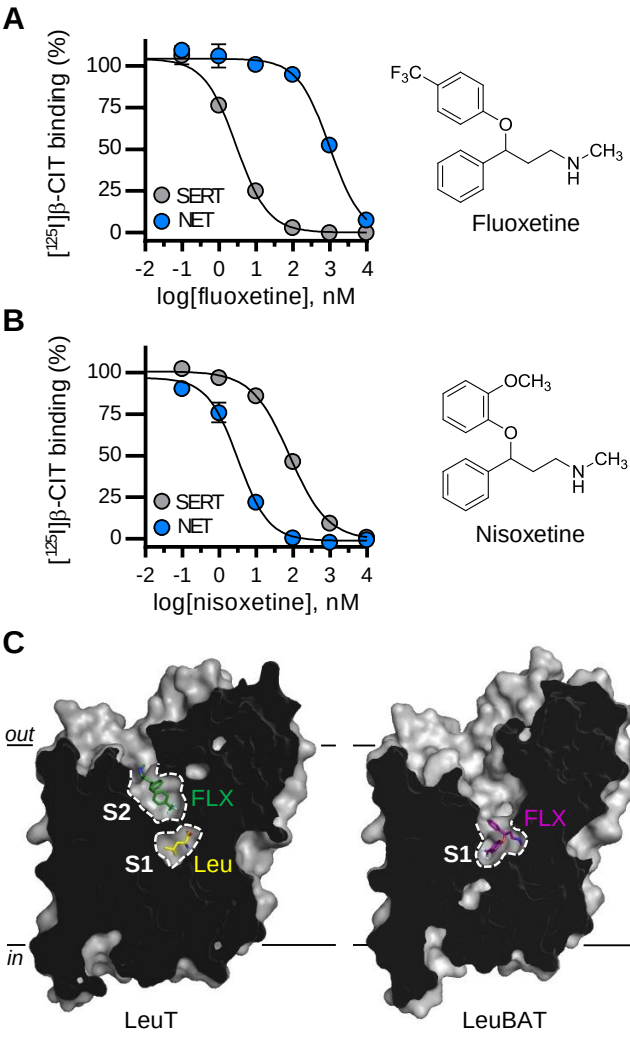
A
[125]β-CIT binding (%)
100
75
50
25
0
SERT
NET
-2 -1 0 1 2 3 4
log[fluoxetine], nM
F3C
O
N
H
CH3
Fluoxetine
B
[125]β-CIT binding (%)
100
75
50
25
0
SERT
NET
-2 -1 0 1 2 3 4
log[nisoxetine], nM
OCH3
O
N
H
CH3
Nisoxetine
C
out
in
S2
FLX
S1
Leu
LeuT
FLX
S1
LeuBAT

Figure 2.

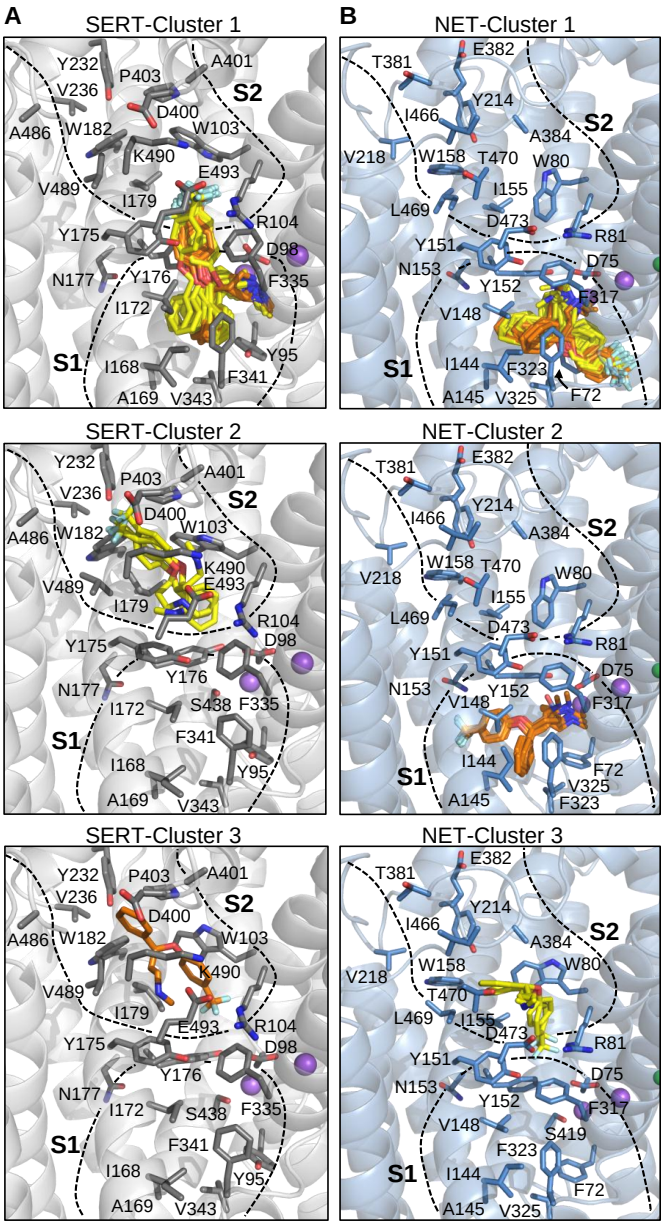
A
SERT-Cluster 1
Y232
P403
A401
V236
S2
D400
A486
W182
W103
K490
E493
V489
I179
R104
Y175
D98
N177
Y176
F335
I172
S1
Y95
I168
F341
A169
V343
SERT-Cluster 2
Y232
P403
A401
V236
S2
D400
A486
W182
W103
K490
E493
V489
I179
R104
Y175
D98
Y176
N177
I172
S438
F335
S1
F341
I168
Y95
A169
V343
SERT-Cluster 3
Y232
P403
A401
V236
S2
D400
A486
W182
W103
K490
V489
I179
E493
R104
Y175
D98
Y176
N177
I172
S438
F335
S1
F341
I168
Y95
A169
V343
B
NET-Cluster 1
E382
T381
Y214
I466
S2
A384
V218
W158
T470
W80
I155
L469
D473
R81
Y151
N153
D75
Y152
F317
V148
S1
I144
F323
A145
V325
F72
NET-Cluster 2
E382
T381
Y214
I466
S2
A384
W158
T470
V218
W80
I155
L469
D473
R81
Y151
D75
N153
Y152
V148
F317
S1
I144
F72
V325
A145
F323
NET-Cluster 3
E382
T381
Y214
I466
S2
A384
V218
W158
W80
T470
L469
I155
D473
R81
Y151
D75
N153
Y152
F317
V148
S419
F323
S1
I144
F72
A145
V325

Figure 3.

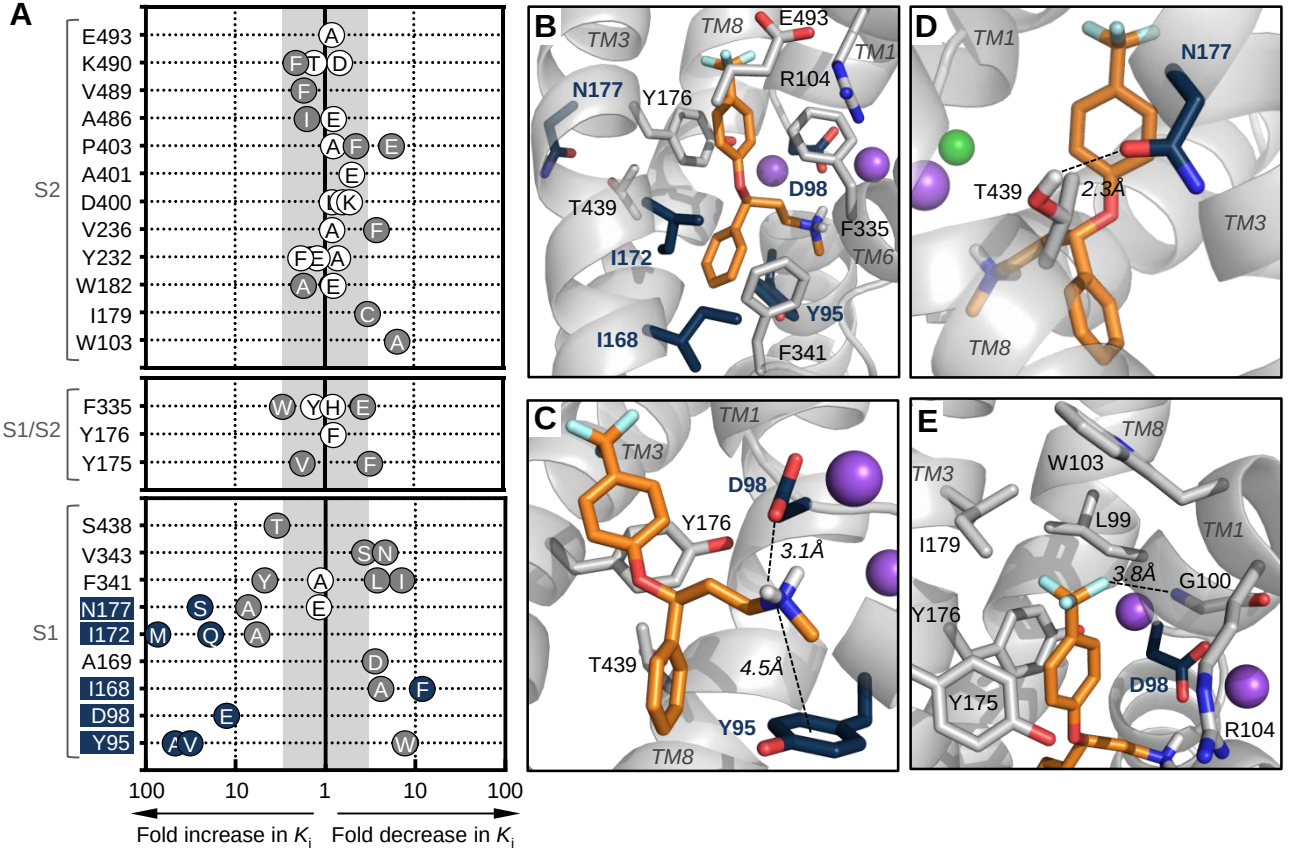
A
S2
E493
K490
V489
A486
P403
A401
D400
V236
Y232
W182
I179
W103
S1/S2
F335
Y176
Y175
S1
S438
V343
F341
N177
I172
A169
I168
D98
Y95
100
10
1
10
100
Fold increase in K_i
Fold decrease in K_i
B
TM3
TM8
E493
TM1
N177
Y176
R104
D98
T439
F335
I172
TM6
Y95
I168
F341
C
TM1
TM3
D98
Y176
3.1Å
T439
4.5Å
Y95
TM8
D
TM1
N177
T439
2.3Å
TM3
TM8
E
TM8
W103
TM3
L99
TM1
I179
3.8Å
G100
Y176
D98
Y175
R104

Figure 4.

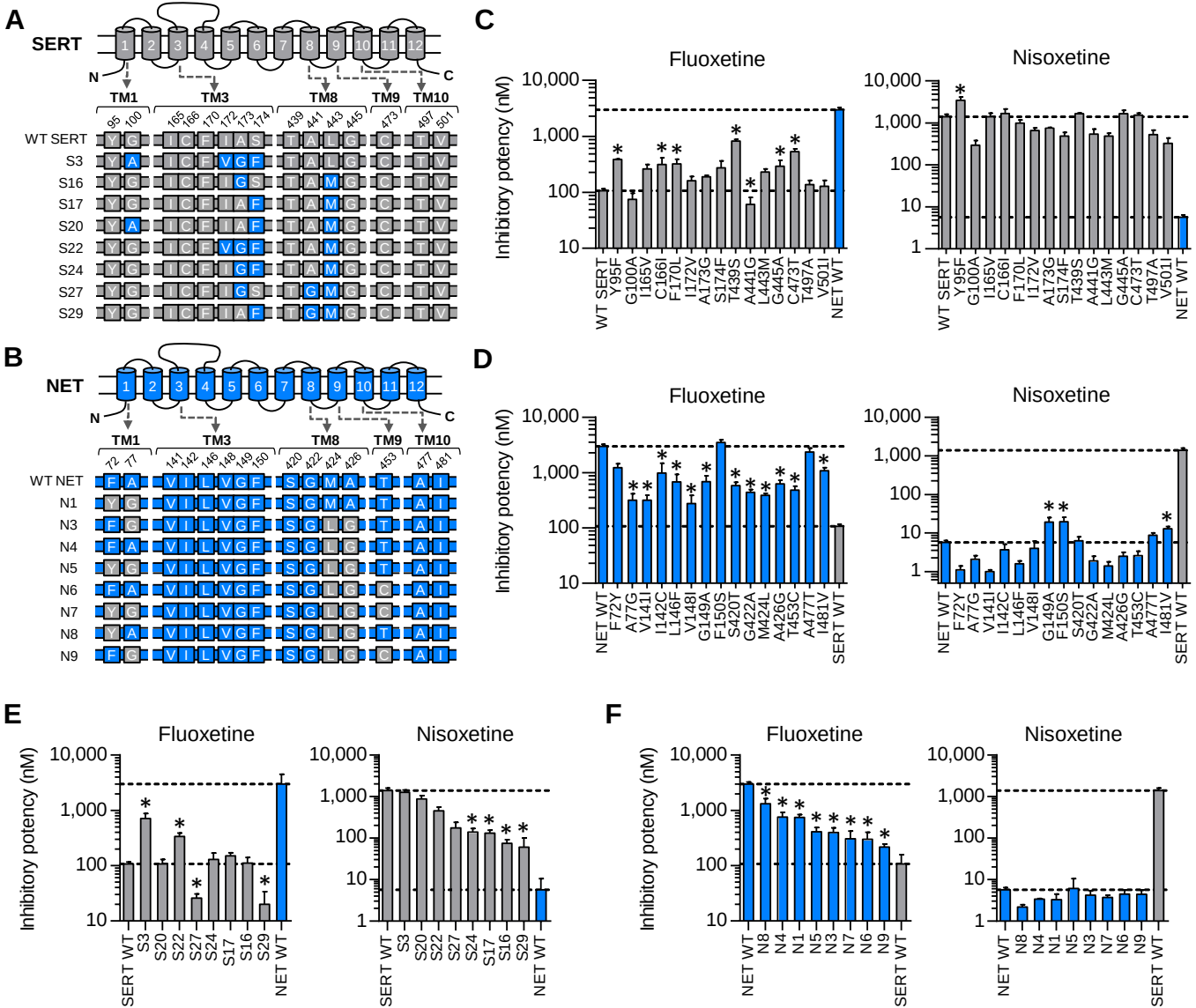
A
SERT
N
C
TM1
TM3
TM8
TM9
TM10
95 100 165 166 170 172 173 174 439 441 443 445 473 497 501
WT SERT Y G I C F I A S T A L G C T V
S3 Y A I C F V G F T A L G C T V
S16 Y G I C F I G S T A M G C T V
S17 Y G I C F I A F T A M G C T V
S20 Y A I C F I A F T A M G C T V
S22 Y G I C F V G F T A M G C T V
S24 Y G I C F I G F T A M G C T V
S27 Y G I C F I G S T G M G C T V
S29 Y G I C F I A F T G M G C T V
B
NET
N
C
TM1
TM3
TM8
TM9
TM10
72 77 141 142 146 148 149 150 420 422 424 426 453 477 481
WT NET F A V I L V G F S G M A T A I
N1 Y G V I L V G F S G M A T A I
N3 F G V I L V G F S G L G T A I
N4 F A V I L V G F S G L G T A I
N5 Y G V I L V G F S G L G T A I
N6 F A V I L V G F S G L G C A I
N7 Y G V I L V G F S G L G C A I
N8 Y A V I L V G F S G L G T A I
N9 F G V I L V G F S G L G C A I
C
Fluoxetine
Nisoxetine
Inhibitory potency (nM)
10,000
1,000
100
10
1
WT SERT Y95F G100A I165V C166I F170L I172V A173G S174F T439S A441G L443M G445A C473T T497A V501I NET WT
D
Fluoxetine
Nisoxetine
Inhibitory potency (nM)
NET WT F72Y A77G V141I I142C L146F V148I G149A F150S S420T G422A M424L A426G T453C A477T I481V SERT WT
E
Fluoxetine
Nisoxetine
Inhibitory potency (nM)
SERT WT S3 S20 S22 S27 S24 S17 S16 S29 NET WT
F
Fluoxetine
Nisoxetine
Inhibitory potency (nM)
NET WT N8 N4 N1 N5 N3 N7 N6 N9 SERT WT

Figure 5.

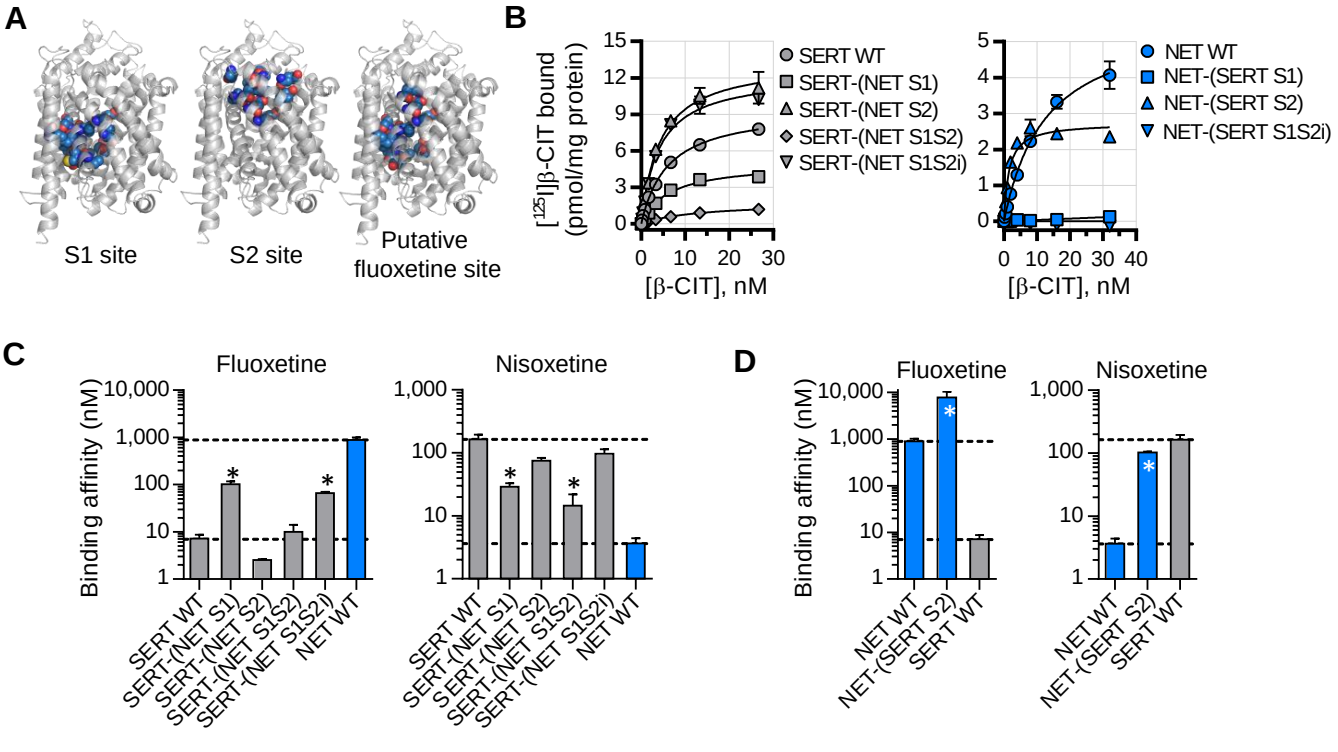
A
S1 site
S2 site
Putative fluoxetine site
B
[125]β-CIT bound (pmol/mg protein)
[β-CIT], nM
SERT WT
SERT-(NET S1)
SERT-(NET S2)
SERT-(NET S1S2)
SERT-(NET S1S2i)
NET WT
NET-(SERT S1)
NET-(SERT S2)
NET-(SERT S1S2i)
C
Fluoxetine
Nisoxetine
Binding affinity (nM)
SERT WT
SERT-(NET S1)
SERT-(NET S2)
SERT-(NET S1S2)
SERT-(NET S1S2i)
NET WT
D
Fluoxetine
Nisoxetine
NET WT
NET-(SERT S2)
SERT WT

Figure 6

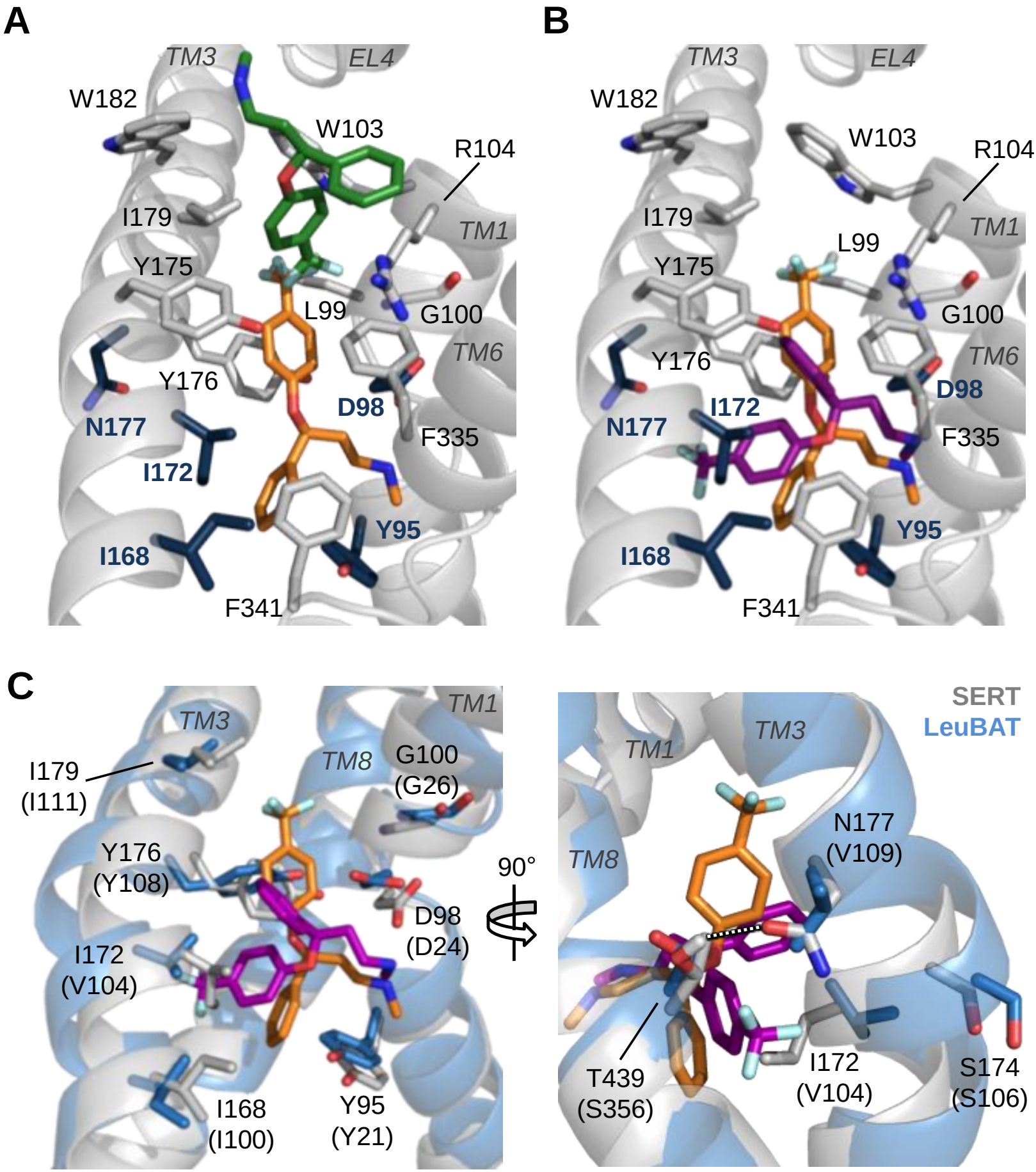
A
TM3
EL4
W182
W103
R104
I179
TM1
Y175
L99
G100
TM6
Y176
D98
N177
F335
I172
Y95
I168
F341
B
TM3
EL4
W182
W103
R104
I179
TM1
L99
Y175
G100
TM6
Y176
D98
I172
N177
F335
Y95
I168
F341
C
TM1
TM3
TM8
I179
(I111)
G100
(G26)
Y176
(Y108)
D98
(D24)
I172
(V104)
90°
I168
(I100)
Y95
(Y21)
SERT
LeuBAT
TM1
TM3
TM8
N177
(V109)
T439
(S356)
I172
(V104)
S174
(S106)